Enzyme and Microbial Technology 57 (2014) 69–77

Contents lists available at ScienceDirect

Enzyme and Microbial Technology

journal homepage: www.elsevier.com/locate/emt

Construction of glutamate biosensor based on covalent immobilization of glutmate oxidase on polypyrrole nanoparticles/polyaniline modified gold electrode

Bhawna Batra, Seema Kumari, Chandra Shekhar Pundir*

Department of Biochemistry, M D University, Rohtak 124001, India

ARTICLE INFO

Article history:
Received 11 October 2013
Received in revised form 23 January 2014
Accepted 1 February 2014
Available online 9 February 2014

Keywords:
Glutamate
Glutamate oxidase
Glutamate biosensor
Polyaniline
Polypyrrole nanoparticles
Food stuff

ABSTRACT

A method is described for construction of a highly sensitive electrochemical biosensor for detection of glutamate. The biosensor is based on covalent immobilization of glutamate oxidase (GluOx) onto polypyrrole nanoparticles and polyaniline composite film (PPyNPs/PANI) electrodeposited onto Au electrode. The enzyme electrode was characterized by cyclic voltammetry (CV), scanning electron microscopy (SEM), X-ray diffraction (XRD), transmission electron microscopy (TEM), Fourier transform infra-red spectroscopy (FTIR) and electrochemical impedance spectroscopy (EIS). The biosensor showed optimum response within 3 s at pH 7.5 (0.1 M sodium phosphate) and 35 °C, when operated at 50 mV s^{-1}. It exhibited excellent sensitivity (detection limit as 0.1 nM), fast response time and wider linear range (from 0.02 to 400 μM). Analytical recovery of added glutamate (5 mM and 10 mM) was 95.56 and 97%, while within batch and between batch coefficients of variation were 3.2% and 3.35% respectively. The enzyme electrode was used 100 times over a period of 60 days, when stored at 4 °C. The biosensor measured glutamate level in food stuff, which correlated well with a standard colorimetric method ($r = 0.99$).

1. Introduction

Glutamate (Glu) is one of the 22 amino acids, which are used to synthesize proteins and takes part in typical metabolic functions like energy production and ammonia detoxification. Glutamate is probably best known as "monosodium glutamate (monosodium salt)" or "MSG" which is employed as a flavor or taste enhancer in food. It is usually available together with other food additives and spices in most large food stores, to give a taste known as Umami. The excessive intake of it simulates glutamate receptors in CNS of vertebrates & thereby release glutamate from neurons which lead to neuronal degeneration & cell death beside several neurological disorders including stroke, epilepsy, Alzheimer's diseases & Parkinson's disease as well as learning & memory power [1–6]. It has also been linked to Chinese Restaurant Syndrome (CRS) [7], being a common ingredient of Chinese food [8]. The term "Chinese restaurant syndrome" is a sudden fall in blood pressure with subsequent fainting after ingestion of very spicy food which is rich in MSG. Hence, there is need to determine its presence in variety of foods. India's Prevention of Food Adulteration Act has set an upper limit of MSG in food, which is 1% [9]. Different techniques have been developed to determine Glu, e.g. potentiometric titration [10], chromatographic [11–15], spectrophotometric [16–18] and fluorimetric [19–22], but these methods require time consuming sample preparation, costly equipment and skilled persons to operate. Biosensors overcome these drawbacks, as these are simple, sensitive, rapid and specific. Recently biosensors have been improved using combination of nanomaterials and conducting polymers.

Polypyrrole, obtained by polymerization of pyrrole is a conducting polymer. The film of polypyrrole is of yellow in color but get darken in air due to oxidation. Although polypyrrole is an insulator, its oxidized derivatives are good electrical conductor with a conductivity range of 2–100 S cm^{-1} [23]. Nanoparticles of polypyrrole have shown the higher conductivity when doped with short alkyl chain than long alkyl chain [24] due to large surface area for reactions and highly porous in sol form [25,26]. PPyNPs sandwiched with core shell Fe_3O_4 nanoparticles have been recently used to improve the analytic performance of potentiometric glucose biosensor [27]. Similarly polyanilne (PANI) is also a polymer of aniline, which has been used in biosensor architecture as transducer, due to its electronic & biomolecular properties [28,29]. The present work describes a unique approach of immobilizing glutamate oxidase onto PPyNPs/PANI, modified Au electrode and its application in construction of an amperometric biosensor for the determination

* Corresponding author at: Department of Biochemistry, M D University, Rohtak 124001, Haryana, India. Tel.: +91 9416492413; fax: +91 126274640.
E-mail addresses: pundircs@rediffmail.com, chandraspundir@gmail.com (C.S. Pundir).

0141-0229/$ – see front matter © 2014 Elsevier Inc. All rights reserved.
http://dx.doi.org/10.1016/j.enzmictec.2014.02.001

of L-glutamte. PPyNPs/PANI, based glutamate biosensor is expected to provide high sensitivity, high biocompatibility, high charge transfer rate and good stability.

2. Experimental

2.1. Materials

Glutamate oxidase (GluOx) from Sigma–Aldrich, St. Louis, USA, potassium ferrocynide ($K_2Fe_2CN_2$) & potassium ferricynide ($K_2(FeCN)_6{\cdot}3H_2O$), aniline, sodium dodecylsulfate (SDS) ($(NH_4)_2S_2O_8$), APS and polypyrrole, and potassium chloride (KCl), from SISCO Research Lab., Mumbai, India, Glutamic acid & Glutraldehyde from LOBA cheme. PVT. LTD. Mumbai, were used. Double distilled water (DW) was used throughout the experimental studies.

2.2. Apparatus used

Potentiostat/Galvanostat (Autolab, model: AUT83785, manufactured by Eco Chemie) with a three electrode system composed of a Pt wire as an auxillary electrode, an Ag/AgCl electrode as reference electrode and GluOx/PPyNPs/PANI/Au electrode as a working electrode. Transmission electron microscope (TEM) (JEOL 2100F) and Scanning electron microscope (SEM) (Zeiss EV040). UV Spectrophotometer (Shimadzu, Model 160A), X-ray diffractometer (XRD), (122 Rigaku, D/Max2550, Tokyo, Japan) Fourier transform infra-red spectrophotometer (FTIR) (Thermo Scientific, USA).

2.3. Assay of free GluOx

The assay of free GluOx was carried out as described by Satyapal and Pundir (1993) [30] with modification. The assay was based on quantification of H_2O_2, generated from oxidation of glutamic acid catalyzed by GluOx, using a color reaction consisting of 4-aminophenazone, phenol and peroxidase as chromogenic system [31]. The reaction mixture containing 1.8 ml of sodium phosphate buffer pH 7.5 (0.1 M), 0.1 ml of L-glutamate solution (1 mM), 0.1 ml of Glu Ox solution (5 U/ml) was incubated at 37 °C for 10 min. One ml of color reagent was added and incubated it in dark at 37 °C for 20 min to develop the color, A_{520} was read and H_2O_2 concentration was extrapolated from its standard curve. One unit of enzyme is defined as amount of enzyme required to catalyze the formation of 1.0 nmol of H_2O_2 from oxidation of glutamate per min/ml under standard assay conditions.

Preparation of color reagent: the color reagent was prepared according to the method of Bais et al. (1980) [30] consisted of 50 mg of 4-aminophenazone, 100 mg solid phenol and 1 mg horseradish peroxidase per 100 ml of 0.4 M sodium phosphate buffer, pH 7.0. It was stored in amber colored bottle at 4 °C and discarded after one week.

2.4. Preparation of PPyNPs

PPyNPs were prepared by microemulsion method [24]. An aqueous solution of 0.08 M SDS was prepared & stirred vigorously for 20 min, then pyrrole was added & stirred vigorously for 30 min. Alcohol was added. After 24 h, excessive methanol was added to terminate the reaction. The precipitate was centrifuged at 5000 rpm for 15–20 min, washed it with methanol, DW & finally with acetone. The PpyNPs were generated, filtered, dried & kept in dessicator.

2.5. TEM of PPyNPs

The morphological characterization of the PPy nanoparticles was carried out in a Transmission electron microscope, at J.N. University, New Delhi.

2.6. Electrodeposition of PPyNPs/PANI onto gold electrode

The surface of Au electrode (2 cm × 1 mm) was polished manually by alumina slurry (diameter 0.05 μm) with a polishing cloth, followed by thorough washing with DW and then placed into ethanol, sonicated to remove adsorbed particles and finally washed with DW for 3–4 times. Aniline (200 μl) and PPyNPs suspension (200 μl) was added into 25 ml of 1 M H_2SO_4 and co-electropolymerized them onto surface of Au electrode through cyclic voltammetry in a potentiostat–galvanostat by applying 50 successive polymerization cycles at −0.3 to 0.7 V at a scan rate of 20 mV s^{-1} (Fig. 1). The resulting PPyNPs/PANI modified Au electrode was washed thoroughly with DW to remove unbound matter and kept in a dry Petri-plate at 4 °C.

2.7. Immobilization of GluOx onto PPyNPs/PANI modified Au electrode

PPyNPs/PANI/Au electrode was immersed into 1 ml of 2.5% glutaraldehyde in 0.05 M sodium phosphate buffer (pH 7.5) for 30 min & then washed thoroughly in 0.05 M sodium phosphate buffer pH 7.5. The glutaraldehyde activated PPyNPs/PANI/Au electrode was dipped into 1.5 ml of GluOx solution (5 U/ml) in 0.1 M sodium phosphate buffer (pH 7.5) and kept overnight at room temperature for immobilization. The resulting electrode with immobilized GluOx was washed 3–4 times with 0.1 M sodium phosphate buffer, pH 7.5 to remove residual unbound protein. The resulting GluOx/PPyNPs/PANI/Au electrode was used as working electrode and stored at 4 °C when not in use. This working electrode was characterized by SEM at different stages of its construction.

2.8. Scanning electron microscopy of Gluox/PPyNPs/PANI/AuE

The SEM images of bare Au electrode, PpyNPs/PANI/Au and GluOx/PPyNPs/PANI/Au electrode were taken in a scanning electron microscope (Zeiss EV040) at J.N. University, New Delhi on commercial basis.

2.9. Construction and testing of glutamate biosensor

An amperometric L-glutamate biosensor was constructed by connecting with Ag/AgCl as reference electrode, GluOx/PPyNPs/PANI/AuE (working electrode) and Pt wire as counter electrode through potentiostat. The CV of this biosensor was recorded in a 25 ml of 0.1 M sodium phosphate buffer (pH 7.4) containing 100 μl of 1 mM glutamate in the range of 0.05–0.5 V at a scan rate of 50 mV s^{-1}.

2.10. Optimization of glutamate biosensor

To optimize working conditions of the biosensor, effects of pH, incubation temperature, time and substrate (Glutamic acid)

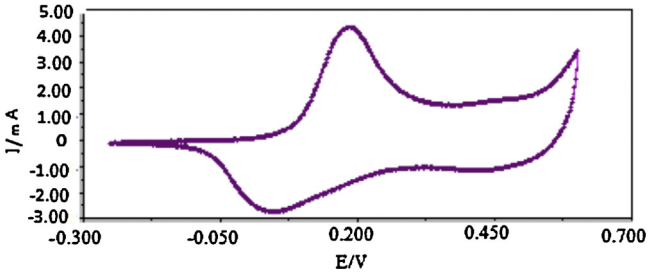

Fig. 1. Cyclic voltamogram for electrodeposition of PPyNPs/PANI composite film. Supporting electrolyte: 1 M H_2SO_4 solution; scan rate: 20 mV s^{-1}.

concentration on biosensor response were studied. To determine optimum pH, the pH was varied between pH 5.5 and 9.5 at an interval of pH 0.5 using the following buffer, each at a final concentration of 0.1 M: pH 5.5 sodium acetate buffer, 6.5–7.5 sodium phosphate buffers, pH 8.0–8.5 Tris HCl buffer and 9–9.5 sodium glycine buffer. Similarly to determine optimum temperature the reaction mixture was incubated at different temperatures (20–50 °C) at an interval of 5 °C. The effect of glutamic acid concentration on biosensor response was determined by varying the concentration of glutamic acid in the range 0.02–1000 μM.

2.11. Application of glutamate biosensor in food stuffs

Food samples (1 ml each) were drawn from ripened tomato, noodles, and tomato soup. Glutamic acid content in food was determined by the present biosensor in the similar manner as described above for its response measurement, under its optimal working conditions except that glutamic acid was replaced by food sample. The glutamic acid content in food was interpolated from standard curve between glutamic acid concentration vs current in μA prepared under optimal assay conditions of GluOx/PPyNPs/PANI/Au enzyme electrode (Fig. 2).

2.12. Interference study

For interference study, following interferents such as citric acid, ascorbic acid, cysteine, methionine, Lysine, aspartic acid, glucose, NaCl, glycine: were added in the reaction mixture individually each at final concentration of 1 mM. The biosensor response, i.e. current (μA) was measured and compared with that where none was added (control) and % relative response was calculated considering the control as 100%.

2.13. Storage stability of GluOx/PPyNPs/PANI/Au electrode

The stability of the working electrode was studied for 4 months by performing the assay on weekly basis. The present electrode system was stored in dried condition at 4 °C, when not in use.

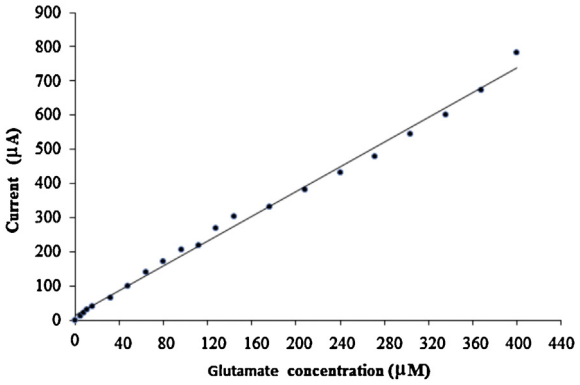

Fig. 2. Standard curve for glutamate biosensor for effect of glutamate concentration on response of glutamate biosensor based on PPyNPs/PANI electrode bound glutamate oxidase.

3. Results and discussion

3.1. Characterization of PPyNPs

The characterization of polypyrrole nanoparticles was carried out by recording its UV and visible spectra, X-ray diffraction (XRD) pattern, transmission electron micrograph (TEM) and Fourier transform infra red spectroscopy (FTIR). The UV and visible spectra exhibited strong absorbance peak at 440 nm, confirming the synthesis of PPyNPs (Fig. 3A). The XRD patterns of PPyNPs clearly showed its characteristics peak at (Fig. 3B). No characteristic peaks of impurities were observed, revealing the high purity of the PPyNPs. The typical TEM images of PPyNPs nanoparticles showed the spherical shape of PPy nanoparticles with an average size of 60–90 nm in diameter (Fig. 3C). The peaks at 1550 and 1475 cm^{-1} corresponded to the stretching vibration of C=C and C—N of PPy respectively. The peak at 1190 cm^{-1} is attributed to bending vibration of the pyrrole ring. The bands of C—H and N—H in-plane deformation vibration are located at 1037 cm^{-1} while the band of C—H out-of-plane deformation vibration was found at 901 cm^{-1}. The expected peak of the S=O stretching vibration of SO^{3-} at

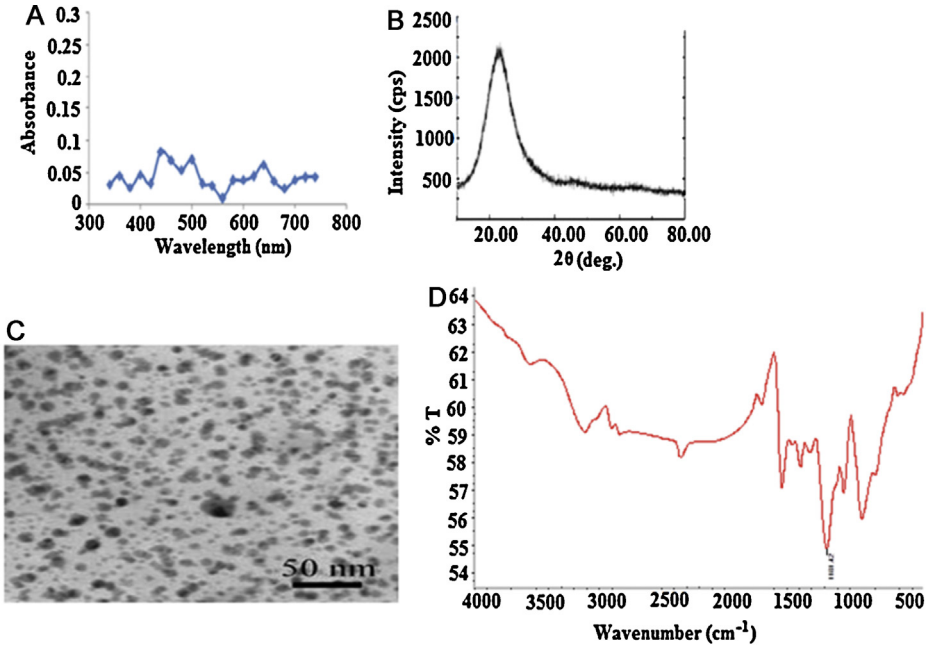

Fig. 3. UV–vis spectra of (A) PPyNPs/PANI, (B) X-ray diffraction (XRD) pattern of PPyNPs/PANI, (C) transmission electron microscopic (TEM) image of PPyNPs/PANI.

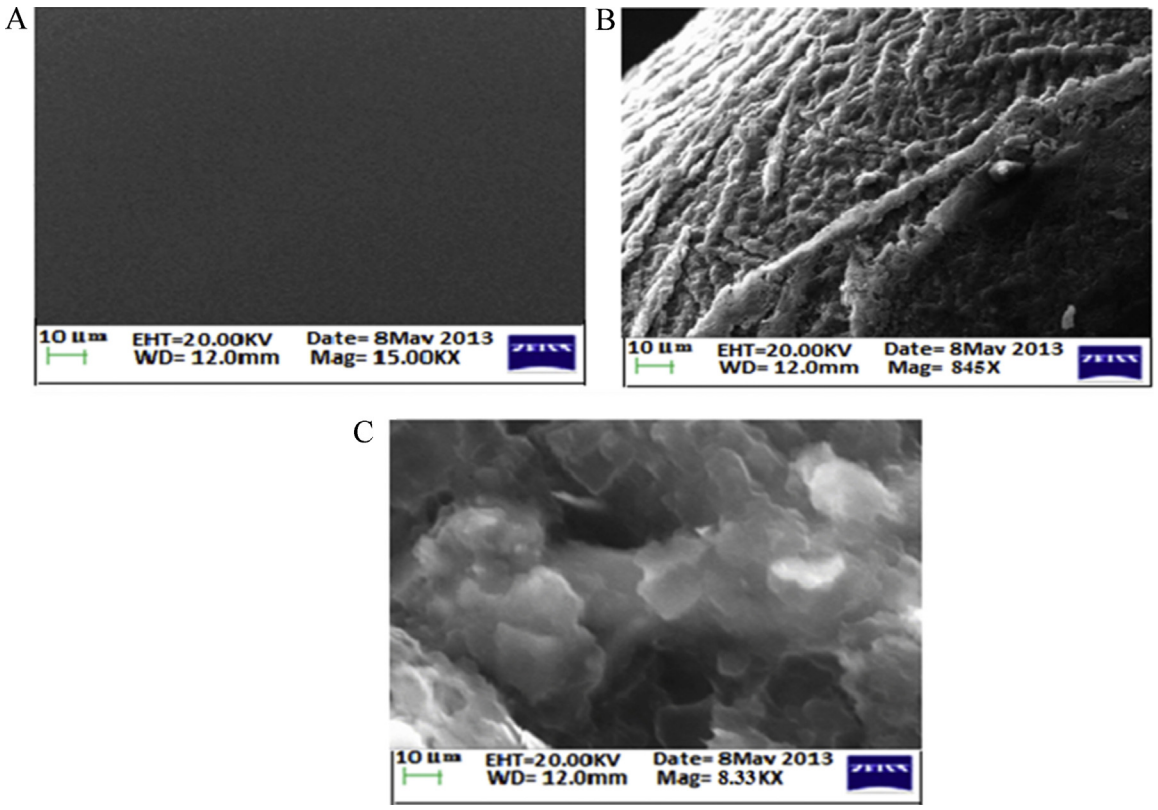

Fig. 4. SEM images of (a) bare Au electrode, (b) PPyNPs/PANI/Au, (c) GluOx/PPyNPs/PANI/Au electrode.

1183 cm^{-1} could not be clearly observed due to overlapping with the pyrrole ring vibration at 1190 cm^{-1} (Fig. 3D).

3.2. SEM studies of Au electrode during its modification

The SEM images of the surface of bare Au electrode, PPyNPs/PANI/Au electrode and GluOx/PPyNPs/PANI/Au electrode are shown in Fig. 4(A–C) respectively. The stepwise modification of electrode could be seen clearly from these SEM images. The SEM image of the bare Au electrode showed a smooth and featureless morphology (Fig. 4A). The PPyNPs/PANI/Au composite film exhibited a net structure. Film was more uniform and porous (Fig. 4B), hence effective surface area is larger. On immobilization of GluOx, the globular structural morphology appeared due to the immobilization of GluOx onto PPyNPs/PANI/Au electrode (Fig. 4C).

3.3. Construction of glutamate biosensor

Fig. 5 summarizes the construction of enzyme electrode based on covalent immobilization of GluOx on PPyNPs decorated PANI film electrodeposited onto surface of Au electrode. PANI and PPyNPs were co-electropolymerised on the surface of Au electrode,

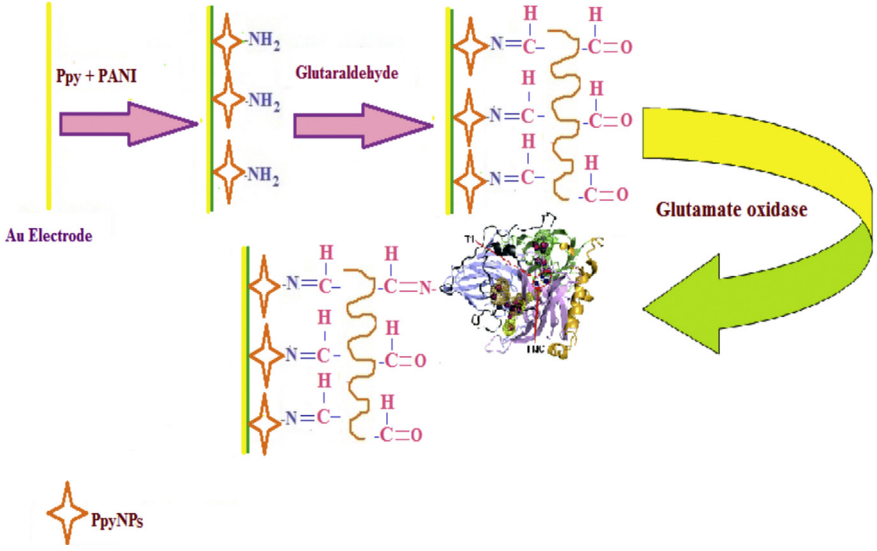

Fig. 5. Schematic representation of chemical reaction involved in the fabrication of GluOx/PPyNPs/PANI/Au electrode.

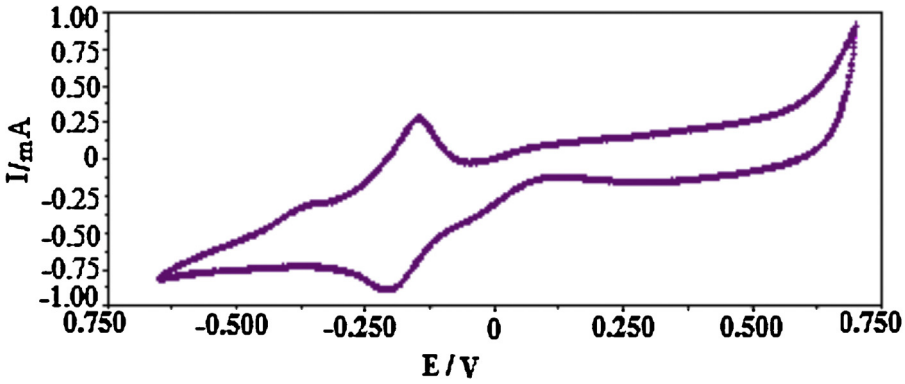

Fig. 6. Cyclic voltammetry response of GluOx/PPyNPs/PANI/Au on successive addition of 100 μl (0.5 mM) glutmate in 25 ml 0.1 M sodium phosphate buffer (pH = 7.5) at the different potential at a scan rate of 50 mV s^{-1}.

as this method is easy and the layer thickness could be controlled. To construct the enzyme electrode, GluOx was immobilized covalently onto PPyNPs/PANI/Au electrode through glutaraldehyde coupling. One —CHO group of glutaraldehyde was linked to —NH_2 group on surface of enzyme, while other —CHO group was bound to —NH_2 group of aniline on PPyNPs–PANI composite film, which provided physically more stable complex. The CVs of PPyNPs/PANI/Au exhibited higher currents than PANI/Au revealing that PPyNPs/PANI/Au composite film, have large effective surface area than PANI/Au composite film and PPyNPs/PANI/Au composite film could provide a conducting path through the composite matrix for faster kinetics. Hence, the PPyNPs acting as electron transfer mediator help in enhancing the biosensor response and thus increases its sensitivity.

3.4. Cyclic voltammetric (CV) studies of glutamate biosensor

The maximum current of the biosensor response (in mA) was observed at −0.130 V (Fig. 6) and hence subsequent studies were carried out at this voltage. Amperometric response of GluOx/PPyNPs/PANI/Au get increased by the addition of 100 μl (1 mM) glutamic acid at the applied potential of −0.130 V. The optimum working potential of present glutamate biosensor was lower than earlier reported amperometric glutamate biosensor based on a on a multilayer of polymer films (+0.085 V) [35], with nanocube and nanosphere augmented single-walled carbon nanotube networks (0.90 V) [41], coupling of GluOx to a copper ion embedded polyion complex membrane (−0.2 V) [43] and functionalized conducting polymer (0.45 V) [44]. The lowering of the working potential in the present biosensor might be due to the presence of PPyNPs/PANI/Au, which provides an environment for the enhanced electrocatalytic effect and a fast electron-transfer rate. The PPyNPs and PANI had a synergistic electrocatalytic effect toward the oxidation of H_2O_2, hence contributes to the excellent performance for the sensor. The existence of PPyNPs and PANI provides a favorable potential window and electrocatalytic behavior for the H_2O_2 electron transfer to the electrode (Table 1).

3.5. FTIR spectra

Fig. 7 showed FTIR spectra of PANI/Au electrode (curve i), PPyNPs/PANI/Au electrode (curve ii) and GluOx/PPyNPs/PANI/Au electrode (curve iii). FTIR spectra of electrodeposited PANI/Au showed a band at 3000.17 cm^{-1} due to N—H stretching of the

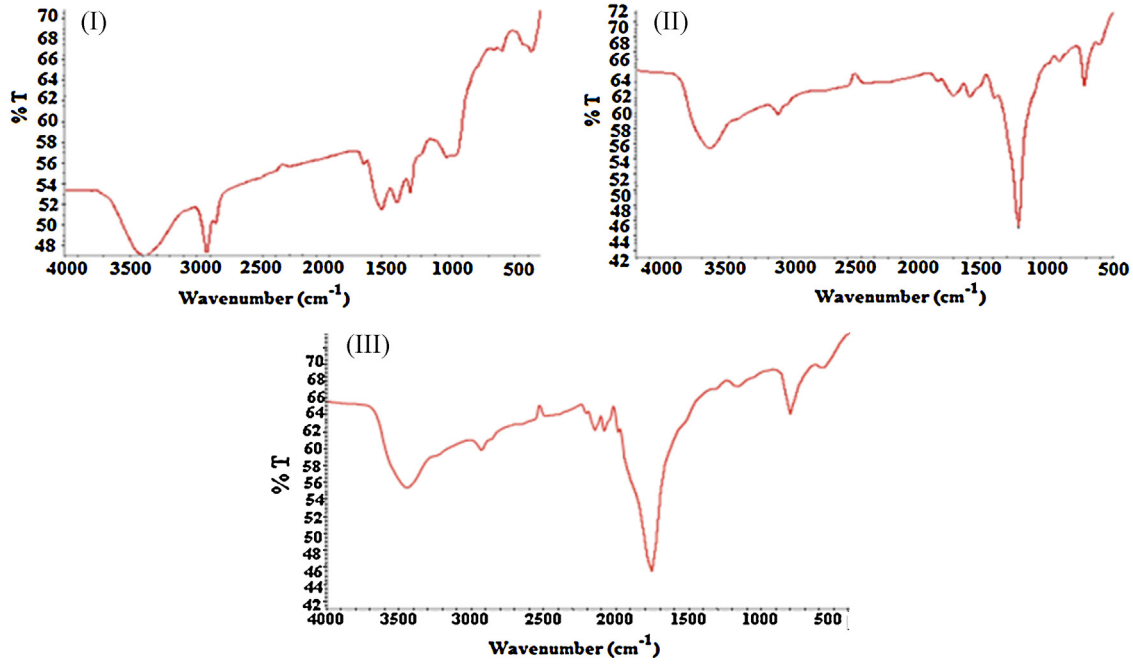

Fig. 7. FTIR spectra of (i) PANI/Au electrode, (ii) PPyNPs/PANI/Au electrode, (iii) GluOx/PPyNPs/PANI/Au electrode.

Table 1
Measurement of apparent K_m for glutamate and sensitivity of GluOx/PPyNPs/PANI/Au electrode at different stages of its construction.

S. no.	Electrode fabrication	App. K_m	Sensitivity (nA/μM/cm^2)
1	GluOx/PANI/Au	254	42
2	GluOx/PPyNPs/Au	245	432
3	GluOx/PPyNPs/PANI/Au	205	533

benzenoid ring. The peak at 1510.52 cm^{-1} is assigned to the quinonoid ring and 1492.80 cm^{-1} is attributed to the benzoid ring (curve i). FTIR spectra of deposited PPyNPs/PANI/Au electrode showed bands at 1550 and 1475 cm^{-1} correspond to the stretching vibration of C=C and C—N of PPy respectively. The peak at 1190 cm^{-1} is attributed to bending vibration of the pyrrole ring. The bands of C—H and N—H in-plane deformation vibration are located at 1037 cm^{-1} while the band of C—H out-of-plane deformation vibration are found at 901 cm^{-1} at 1360 and 3398 cm^{-1} due to the presence of C—N bending and N—H stretching vibrations, respectively (curve ii). The peak at 1762 cm^{-1} is assigned to C—O stretching, while peak at 1549 cm^{-1} is attributed to amide I group (C—O stretching along with N—H deformation mode) as shown in curve iii. This shows the covalent immobilization of GluOx onto PPyNPs/PANI/Au electrode.

3.6. Electrochemical impedance measurements (EIS)

Fig. 8 showed electrochemical impedance spectra (EIS) of (i) bare Au electrode (ii) PPyNPs/PANI/Au electrode and (iii) GluOx/PPyNPs/PANI/Au electrode in containing 5 mM $K_3Fe(CN)_6/K_4Fe(CN)_6$ (1:1) as a redox probe. EIS provided an effective method to probe electronic features of surface-modified electrodes. The R_{CT} values (semicircle diameter) for bare Au electrode, PPyNPs/PANI/Au electrode and GluOx/PPyNPs/PANI/Au electrodes were 970 Ω, 650 Ω and 757 Ω respectively. The R_{CT} of GluOx/PPyNPs/PANI/Au (iii) bioelectrode was higher compared with that of PPyNPs/PANI/Au (ii) electrode. This increase in R_{CT} can be attributed to the fact that most biological molecules, including enzymes, are poor electrical conductors and cause hindrance to electron transfer. These results also indicate the binding of enzymes onto PPyNPs/PANI/Au composite.

3.7. Optimization of biosensor

The experimental conditions affecting the biosensor response were studied in terms of effect of pH, incubation temperature, time and substrate (glutamate) concentration. The optimum current was obtained at pH 7.5, which is near to that of earlier reported L-glutamate biosensors (Table 2). The optimum temperature of the present biosensor was at 35 °C which is higher to earlier reported biosensors but similar to one biosensor (Table 2). The current response decreased rapidly after 40–50 °C due to thermal inactivation of the enzyme. Hence, the subsequent experiments were performed at 35 °C. The biosensor showed optimum response within 3 s, which is lower than earlier glutamate biosensors (Table 2). There was a hyperbolic relationship between biosensor response and glutamic acid concentration range 0.02–1000 μM with the linearity up to 400 μM. The app K_m value for the present enzyme electrode was calculated from LB plot and found to be 205 μM, which is lower than those reported for earlier biosensors (Table 2).

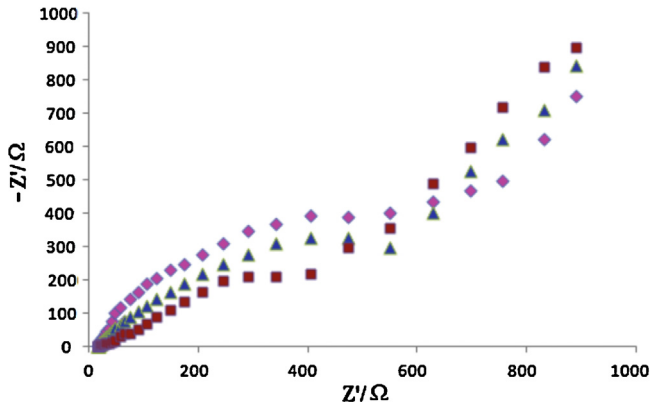

Fig. 8. Impedance spectroscopy study of (i) Bare Au, (ii) PPyNPs/PANI/Au, (iii) GluOx/PPyNPs/PANI/Au in 5 mM $K_3Fe(CN)_6/K_4Fe(CN)_6$ (1:1) as a redox probe.

3.8. Evaluation of biosensor

3.8.1. Linearity

There was a linear relationship between the current (in μA) and the glutamic acid concentration in the range 0.02–400 μM which is wider than earlier reported biosensors (Table 1).

3.8.2. Detection limit

The detection limit of the present sensor was 0.1 nM (S/N = 3) which is better than earlier reported biosensors (Table 1).

3.8.3. Analytical recovery

The average recoveries of glutamic acid added to food stuff (at levels of 5 mM and 10 mM) were 95.5 and 97.0% demonstrating the good reliability of the present biosensor (Table 3).

3.8.4. Precision

Within-sample and between-sample coefficients of variation for the determination of glutamic acid in food on the same day and after one week of storage were 3.2 and 3.35%, respectively. These high precisions highlight the good reproducibility and consistency of the present method, which may be attributed to the covalent immobilization of glutamate oxidase onto the PPyNPs/PANI/Au electrode.

3.8.5. Application of glutamate biosensor

The L-glutamic acid level in following food stuffs such as tomato, noodles and tomato soup was measured by the present biosensor and found to be 256 μM, 312 μM and 365 μM respectively (range 256–365 μM). There was a good correlation (r = 0.997) between these values and the values obtained by standard enzymic colorimetric method (Fig. 9).

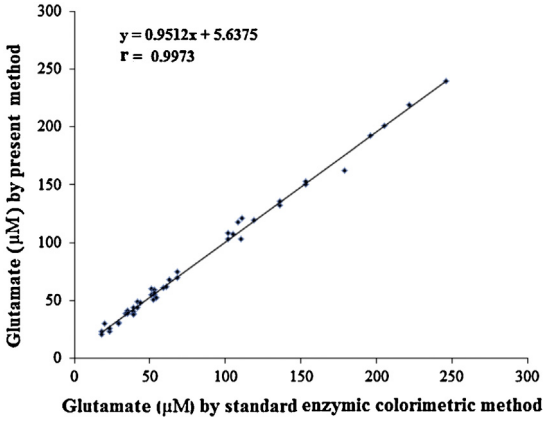

Fig. 9. Correlation between glutamate values measured by enzymic colorimetric (x-axis) and the current method (y-axis) employing the glutamate biosensor based on GluOx/PPyNPs/PANI/Au.

Table 2
A comparison of analytical characteristics of various glutamate biosensors.

Properties	[32]	[33]	[34]	[35]	[36]	[9]	[37]
Source of enzyme	–	*Streptomyces* sp.	–	–	*Streptomyces* sp.	*Streptomyces* sp.	–
Support of immobilization	Teflon-coated Pt wire	Graphite electrode	Nafion film on MnO_2 bulk-modified carbon electrodes	Multilayer of polymer films	Polycarbonate membrane	Polycarbonate membrane	Pt nanoparticle modified ordered three-dimensional gold nanowire arrays (Pt NP/NAEs)
Type of transducer	Amperometric	Amperometric	–	Amperometric	DO metric	DO metric	Amperometric
Methods for immobilization	Adsorption	Cross-linking	Entrapment	Entrapment	Cross-linking	Cross-linking	Cross-linking
Optimum pH	7.4	–	7.75	7.4	6.0	7.0	7.4
Temperature	–	–		–	24	25	–
Linearity	–	1–250 μM	53–855 μM	0.5–8.0 mM	68–1271 μM	0.136–138 μM	–
K_m	–	–	–	–	–	0.4451 mM	–
Detection limit	0.3 μM	0.7 μM	9.12 μM	–	68 μM	0.68 μM	–
Response time	–	–	–	–	120 s	120 s	–
Storage stability	–	–	–	16 days	60 days	–	–
Application	–	–	–	Soy sauce	Food samples	–	–

Properties	[38]	[39]	[40]	[41]	[42]	[6]	Present work
Source of enzyme	–	–	–	–	*Streptomyces* sp.	*Streptomyces* sp.	*Streptomyces* sp.
Support of immobilization	Pt electrode modified with PPy and MWCNT	Tetrafulvalene-tetracyanoquinodimethane (TTF-TCNQ) paste	N-(3-dimethylaminopropyl)-N′-ethylcarbodiimide hydrochloride (EDC) activated thioglycolic acid (TGA) self-assembled monolayer (SAM)	Networks of SWCNTs enhanced with Pd nanocubes and Pt nanospheres	Novel glutamate oxidase integrated into a redox hydrogel	cMWCNT/AuNP/CHIT/Au	PPyNPs/PANI/Au
Type of transducer	Amperometric	Amperometric	–	Amperometric	Amperometric	Amperometric	Amperometric
Methods for immobilization	–	Cross-linking	–	Cross-linking	Cross-linking	Covalent	Covalent
Optimum pH	–	7.0	–	7.4	7–9	7.5	7.5
Temperature	–	25	–		–	35	35
Linearity	Up to 140 μM	–	0.1 μM–10.0 mM	50 nM–1.6 mM	0–500 μM	5–500 μM	0.02–400 μM
K_m	–	–	–	–	5 mM	–	205 μM
Detection limit	0.3 μM	0.05 mM	0.089 μM	4.6 nM	0.5 μM	1.6 μM	0.1 nM
Response time	7 s	20–50 s	–		10	2 s	3 s
Storage stability	–	10 days	–			120 days	60 days
Application	–	Tomato	–	–		Serum	Food stuffs

cMWCNT, carboxylated multiwalled carbon naotubes; AuNP, gold nanoparticles; CHIT, chitosan; SWCNT, single walled carbon nanotubes; PPyNPs, polypyrrole nanoparticles; PANI, polyaniline.

Table 3
Analytical recovery of added glutamic acid in the food samples, as measured by glutamate biosensor based on glutamate oxidase bound to GluOx/PPyNPs/PANI/Au electrode.

Glutamic acid added (mM)	Glutamic acid found (mM)	% Recovery
–	0.153	100
5	4.931	95.56 ± 2.7
10	9.853	97.0 ± 3.1

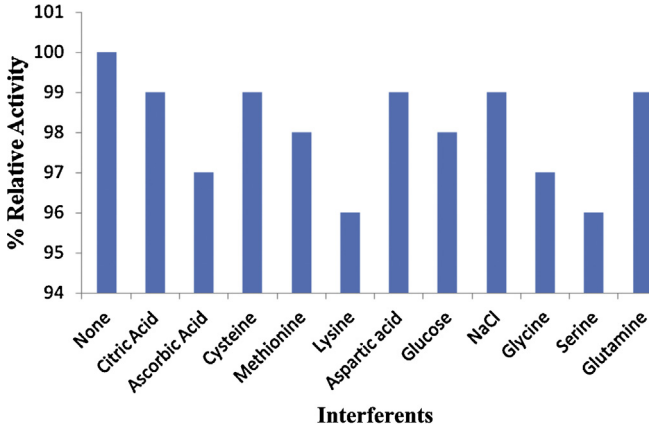

Fig. 10. Effect of potential interferents on response of GluOx/PPyNPs/PANI modified Au electrode.

3.9. Interference study

Among the various substances tested such as citric acid, ascorbic acid, cysteine, methionine, Lysine, aspartic acid, glucose, NaCl, glycine (each at 1 mM), none had practically any interference (Fig. 10).

3.10. Long-term stability of enzyme electrode

The enzyme electrode lost only 30% of its initial activity after its 100 regular uses over a period of 60 days. These observations indicate the better stability of enzyme electrode than earlier enzyme electrodes (Table 1).

4. Conclusion

An improved amperometric bilirubin biosensor was constructed by immobilizing covalently a glutamate oxidase onto PPyNPs/PANI electrodeposited onto Au electrode which exhibited relatively rapid response (3 s), broad linear range (0.02–400 μM), low detection limit (0.1 nM), good reproducibility and long stability (60 days at 4 °C).

Acknowledgements

Author (Bhawna Batra) is thankful to the Council of Scientific and Industrial Research (CSIR), India, for the award of Junior Research Fellowship during this study.

References

[1] Riedel G, Reymann KG. Metabotropic glutamate receptors in hippocampal long-term potentiation and learning and memory. Acta Physiol Scand 1996;157:1–19.
[2] Johnston ANB, Rogers LJ. Right hemisphere involvement in imprinting memory revealed by glutamate treatment. Pharmacol Biochem Behav 1998;60:863–71.
[3] Burmeister JJ, Pomerleau F, Palmer M, Day BK, Huettl P, Gerhardt GA. Improved ceramic-based multisite microelectrode for rapid measurements of L-glutamate in the CNS. J Neurosci Methods 2002;119:163–71.
[4] Hynd MR, Scott HL, Dodd PR. Glutamate-mediated excitotoxicity and neurodegeneration in Alzheimer's disease. Neurochem Int 2004;45:583–95.
[5] Takeda A, Minami A, Sakurada N, Nakajima S, Naoto O. Response of hippocampal mossy fiber zinc to excessive glutamate release. Neurochem Int 2007;50:322–7.
[6] Batra B, Pundir CS. An amperometric glutamate biosensor based on immobilization of glutamate oxidase onto carboxylated multiwalled carbon nanotubes/gold nanoparticles/chitosan composite film modified Au electrode. Biosens Bioelectron 2013;47:496–501.
[7] Schaumburg HH, Byck R, Gerstl R, Mashman JH. Monosodium L-glutamate: its pharmacology and role in the Chinese restaurant syndrome. Science 1969;163:826–8.
[8] Pasco N, Jeffries C, Davies Q, Downard AJ, Roddick-Lanzilotta AD, Gorton L. Characterisation of a thermophilic L-glutamate dehydrogenase biosensor for amperomatric determination of L-glutamate by flow injection analysis. Biosens Bioelectron 1999;14:171–8.
[9] Basu AK, Chattopadhyay P, Roychudhuri U, Chakraborty R. A biosensor based on co-immobilized L-glutamate oxidase and L-glutamate dehydrogenase for analysis of monosodium glutamate in food. Biosens Bioelectron 2006;21:1968–72.
[10] Gunduz T, Gunduz N, Kilic E, Koseoglu F, Guloztas S. Titration in non aqueous media. Part X. Potentiomatric and conductomatric titrations of amino acids with tetrabutylammonium hydroxide in pyridine and acetonitrile solvents. Analyst 1998;113:715–9.
[11] Zhang LY, Sun MX. Selective determination of γ-aminobutyric acid, glutamate and alanine by mixed micellar electrokinetic chromatography and fluorescence detection. J Chromatogr A 2005;1095:85–188.
[12] Clarke G, Mahony SO, Malone G, Dinan TG. An isocratic high performance liquid chromatography method for the determination of GABA and glutamate in discrete regions of the rodent brain. J Neurosci Methods 2007;160:223–30.
[13] Shah AJ, Flor R, Atkins A, Murphy JS, Dawson LA. Development application of a liquid chromatography/tandem mass spectrometric assay for measurement of N-acetylaspartate N-acetylaspartylglutamate glutamate in brain slice superfusates tissue extracts. J Chromatogr B 2008;876:153–8.
[14] Acuna AAM, Trias JF. A high performance liquid chromatography method with electrochemical detection of gamma-aminobutyric acid, glutamate and glutamine in rat brain homogenates. J Neurosci Methods 2009;183:176–81.
[15] Buck K, Voehringer P, Ferger B. Rapid analysis of GABA and glutamate in microdialysis samples using high performance liquid chromatography and tandem mass spectrometry. J Neurosci Methods 2009;182:78–84.
[16] Kampha W, Meevootisom V, Wiyakrutta S. Spectrophotometric enzymatic cycling method using L-glutamate dehydrogenase and D-phenylglycine aminotransferase for determination of L-glutamate in foods. Anal Chim Acta 2004;520:133–9.
[17] Tang L, Zhu Y, Xu L, Yang X, Li C. Amperometric glutamate biosensor based on self-assembling glutamate dehydrogenase and dendrimer-encapsulated platinum nanoparticles onto carbon nanotubes. Talanta 2007;73:438–43.
[18] Acebal CC, Lista AG. Band BSF. Simultaneous determination of flavor enhancers in stock cube samples by using spectrophotometric data and multivariate calibration. Food Chem 2008;106:811–5.
[19] Sanchez FG, Gallardo AA. Liquid chromatographic and spectrofluorimetric determination of aspartame and glutamate in foodstuffs following fluorescamine fluorigenic labelling. Anal Chim Acta 1992;270:45–53.
[20] Tcherkas YV, Denisenko AD. Simultaneous determination of several amino acids including homocysteine cysteine glutamic acid in human plasma by isocratic reversed-phase high-performance liquid chromatography with fluorimetric detection. J Chromatogr A 2001;913:309–13.
[21] Tsukatani T, Matsumoto K. Sequential fluorometric quantification of γ-aminobutyrate and L-glutamate using a single line flow-injection system with immobilized – enzyme reactors. Anal Chim Acta 2005;546:154–60.
[22] Chakraborty S, Raj CR. Amperometric biosensing of glutamate using carbon nanotube based electrode. Electrochem Commun 2007;9:1323–30.
[23] Moghaddam AB, Nazari T, Badraghi J, Kazemzad M. Synthesis of ZnO nanoparticles and electrodeposition of polypyrrole/ZnO nanocomposite film. Int J Electrochem Sci 2009;4:247–57.
[24] Reung-U-Rai A, Prom-Jun A, Prissanaroon-Ouajai W, Ouajai S. Synthesis of highly conductive polypyrrole nanoparticles via microemulsion polymerization. JOM 2008;18:27–31.
[25] Jang J. Conducting polymer nanomaterials their applications. Adv Polym Sci 2006;199:189–260.
[26] Suri K, Annapoorni S, Tandon RP, Rath C, Aggrawal VK. Thermal transition behaviour of iron oxide–polypyrrole nanocomposites. Curr Appl Phys 2003;3:209–13.
[27] Yanga Z, Zhanga C, Zhanga J, Baic W. Potentiometric glucose biosensor based on core–shell Fe_3O_4–enzyme–polypyrrole nanoparticle. Biosens Bioelectron 2014;15:268–73.
[28] Batra B, Lata S, Sharma M, Pundir CS. An acrylamide biosensor based on immobilization of hemoglobin onto multiwalled carbon nanotube/copper nanoparticles/polyaniline hybrid film. Anal Biochem 2013;433:210–7.
[29] Dhand C, Das M, Datta M, Malhotra BD. Recent advances in polyaniline based biosensors. Biosens Bioelectron 2011;26:2811–21.
[30] Satyapal, Pundir CS. Purification & properties of an oxalate oxidase from leaves of grain sorghum hybrid CSH-5. Biochem Biophys Acta 1993;11:611–5.
[31] Bais R, Potezny N, Edward JB, Rofe AM, Conyer R. Oxalate determination by immobilized oxalate oxidase in a continuous flow system. Anal Chem 1980;52:508–11.

[32] Ryan MR, Lowry JP, O'Neill RD. Biosensor for neurotransmitter L-glutamic acid designed for efficient use of L-glutamate oxidase and effective rejection of interference. Analyst 1997;122:1419–24.
[33] Yigzaw Y, Larsson N, Gorton L, Ruzgas T, Solomon T. Liquid chromatographic determination of total and β-N-oxalyl-l-α,β-diaminopropionic acid in *Lathyrus sativus* seeds using both refractive index and bioelectrochemical detection. J Chromatogr A 2001;929:13–21.
[34] Beyene NW, Moderegger H, Kalcher K. Development of an amperometric biosensor for β-ODAP. Electroanalysis 2004;16:268.
[35] Nakorn PN, Suphantharika M, Udomsopagit S, Surareungchai W. Poly(vinylferrocene)–poly(ethylene glycol) glutamate oxidase electrode for determination of L-glutamate in commercial soy sauces. World J Microbiol Biotechnol 2003;19:479–85.
[36] Basu AK, Chattopadhyay P, Roychudhuri U, Chakraborty R. Development of biosensor based on immobilized L-glutamate oxidase for determination of monosodium glutamate in food. Indian J Exp Biol 2006;44:392–8.
[37] Jamal M, Xu J, Razeeb KM. Disposable biosensor based on immobilisation of glutamate oxidase on Pt nanoparticles modified Au nanowire array electrode. Biosens Bioelectron 2010;26:1420–4.
[38] Ammam M, Fransaer J. Highly sensitive and selective glutamate microbiosensor based on cast polyurethane/AC-electrophoresis deposited multiwalled carbon nanotubes and then glutamate oxidase/electrosynthesized polypyrrole/Pt electrode. Biosens Bioelectron 2010;25:1597–602.
[39] Pauliukaite R, Zhylyak G, Citterio D, Spichiger-Keller UE. L-Glutamate biosensor for estimation of the taste of tomato specimens. Anal Bioanal Chem 2006;386:220–7.
[40] Rahman MM. Fabrication of mediator-free glutamate sensors based on glutamate oxidase using smart micro-devices. J Biomed Nanotechnol 2011;7:351–7.
[41] Claussen JC, Artiles MS, McLamore ES, Mohanty S, Shi J, Rickus JL, et al. Electrochemical glutamate biosensing with nanocube and nanosphere augmented single-walled carbon nanotube networks: a comparative study. J Mater Chem 2011;21:11224–31.
[42] Mikeladze E, Collins A, Sukhacheva M, Netrusov A, Csoregia E. Characterization of a glutamate biosensor based on a novel glutamate oxidase integrated into a redox hydrogel. Electroanalysis 2002;14:1052–9.
[43] Hasebe Y, Gu T, Kusakabe H. Glutamate biosensor using a DNA-Cu(II)/polyamine membrane as a novel electrolytic layer for cathodic determination of hydrogen peroxide. Electrochemistry 2006;74:179–82.
[44] Rahman MA, Kwon NH, Won MS, Choe ES, Shim YB. Functionalized conducting polymer as an enzyme-immobilizing substrate: an amperometric glutamate microbiosensor for in vivo measurements. Anal Chem 2005;77:4854–60.